Available online at www.sciencedirect.com

ScienceDirect

Proceedings of the Combustion Institute xxx (2014) xxx–xxx

Proceedings of the Combustion Institute

www.elsevier.com/locate/proci

Performance of conditional source-term estimation model for LES of turbulent premixed flames in thin reaction zones regime

Nasim Shahbazian [a,*], M. Mahdi Salehi [b], Clinton P.T. Groth [a], Ömer L. Gülder [a], W. Kendal Bushe [b]

[a] *Institute for Aerospace Studies, University of Toronto, 4925 Dufferin Street, Toronto, Ontario M3H 5T6, Canada*
[b] *Department of Mechanical Engineering, University of British Columbia, 6250 Applied Science Lane, Vancouver, B.C. V6T 1Z4, Canada*

Abstract

Conditional source-term estimation (CSE) is a subfilter-scale (SFS) model for representing turbulence-chemistry interactions in turbulent reactive flows. In the present study, the CSE model is coupled with a two-dimensional flame-generated manifold (FGM) chemistry reduction technique and modified laminar-flame-based probability density function (PDF) and applied to large eddy simulation (LES) of laboratory-scale turbulent premixed flames. CSE estimates conditional moments by solving an inverse problem and uses a conditional moment closure to determine the influence of the unresolved turbulence on the reaction rates. While the CSE model has been used extensively in simulating turbulent non-premixed flames, the study represents a first application of the combustion model to LES of premixed flames. Two axisymmetric Bunsen-type premixed turbulent methane–air flames are examined corresponding to lean and stoichiometric conditions with both lying within the thin reaction zones regime. The LES predictions are compared to available experimental data for the two flames. The predictions of the CSE model are also compared to those of a more traditional flamelet-based approach: the presumed conditional moment (PCM) with flame prolongation of intrinsic low-dimensional manifolds (FPI) tabulated chemistry, or so-called PCM-FPI model. The comparisons of the CSE and PCM-FPI models allow the relative importance of deviations from the standard flamelet assumption to be assessed for flames lying outside the flamelet premixed combustion regime. The performance of CSE for LES of turbulent premixed combustion is evaluated. The CSE combustion model is found to be stable and converges to physically meaningful values. It also yields LES results that agree very well with experiment, both qualitatively and quantitatively, and would seem able to incorporate correctly the influence of turbulent strain on conditionally-filtered quantities and hence burning rate as flame behaviour deviates from that of a flamelet in the thin reaction zones regime.

Keywords: Conditional source-term estimation (CSE); Large eddy simulation (LES); Turbulent premixed flames

* Corresponding author. Fax: +1 416 667 7799.
E-mail addresses: shahbazian@utias.utoronto.ca (N. Shahbazian), salehi@alumni.ubc.ca (M.M. Salehi), groth@utias.utoronto.ca (C.P.T. Groth), ogulder@utias.utoronto.ca (Ö.L. Gülder), wkb@mail.ubc.ca (W.K. Bushe).

http://dx.doi.org/10.1016/j.proci.2014.06.132
1540-7489/

Please cite this article in press as: N. Shahbazian et al., *Proc. Combust. Inst.* (2014), http://dx.doi.org/10.1016/j.proci.2014.06.132

1. Introduction

Large eddy simulation (LES) is a powerful computational tool for modelling turbulent reactive flows. However, a considerable complication for LES of turbulent premixed combustion is that the flame thickness is generally much smaller than the LES filter width such that reaction zones and flame fronts cannot be resolved on the grids. Accurate subfilter-scale (SFS) models of the unresolved turbulence-chemistry interactions are therefore required. Unfortunately, there are as yet no universal models that fully account for the SFS turbulence-chemistry interactions and predict the observed flame behaviour.

Many different models have been proposed for turbulence-chemistry interactions. These models range from simple eddy break-up models [1] to flamelet models [2–8], conditional moment closure (CMC) [9], and transported probability density function (PDF) models [10,11]. Eddy break-up models are simple algebraic models that are generally not as accurate as other models. The limiting assumption of flamelet models is that the flame is thin and locally laminar, which becomes questionable away from the traditional flamelet regime [12]. CMC is a more general approach as compared to flamelet models. Conditional moments are used to close the chemical reaction source terms; however, the transport equations for these conditional averages have several unclosed terms. These require modelling and there are uncertainties in their treatment. Transported PDF models theoretically can provide a "perfect" closure for chemical reaction source terms; however, the transport equation for the joint PDF of the scalars/scalars-velocity is unclosed and closure models are still needed.

In this study, the conditional source-term estimation (CSE) combustion model of Bushe and Steiner [13,14] has been implemented as a LES SFS model for turbulent premixed combustion following a similar procedure outlined previously for Reynolds-averaged Navier–Stokes (RANS) computations and *a priori* DNS of premixed flames [15,16]. The CSE model is a CMC-based model that utilizes the CMC hypothesis to represent turbulence-chemistry interactions. The difference between CSE and CMC models is that unlike CMC, in CSE, transport equations are not solved for the conditional scalar field. A dynamic approach is used to obtain these quantities via solution of an inverse problem. Here, a reduced chemical kinetic model, based on a two-dimensional flame-generated manifold (2D-FGM) approach [17,18], and modified laminar flamelet presumed PDF [19,20], was coupled with the CSE model and applied to LES of several laboratory-scale turbulent premixed flames. While the CSE model has been used previously in simulating turbulent non-premixed flames [13,14,17,21,22] and for RANS simulations and *a priori* DNS of premixed combustion [15,16,23], the present work represents a first application of this combustion model to LES of premixed flames. Two axisymmetric Bunsen-type premixed turbulent methane–air flames were examined, corresponding to lean and stoichiometric conditions, and the LES predictions are compared to available experimental data of Yuen and Gülder [24]. The predictions of the CSE model were also compared to those of a more traditional flamelet-based approach: the presumed conditional moment (PCM) with flame prolongation of intrinsic low-dimensional manifolds (FPI) tabulated chemistry [4], or so-called PCM-FPI model [6–8]. The two flames of interest both lie within the thin reaction zones regime of the regime diagram for premixed flames [12] and therefore allowed the relative importance of deviations from the standard flamelet assumption to be assessed for flames outside the flamelet regimes. The capabilities of the CSE combustion model to predict observed behaviour were assessed and the findings are discussed.

2. LES framework

The LES framework developed by Hernández-Pérez et al. [25] was used in performing this study. The Favre-filtered form of the Navier–Stokes equations governing compressible flows of a thermally perfect reactive mixture of gases, neglecting Dufour, Soret and radiation effects, were solved. Thermodynamic and molecular transport properties of each mixture component were prescribed using the database compiled by Gordon and McBride [26]. The SFS turbulent viscosity was modelled using k-equation model [27]. Other SFS scalar fluxes were closed using standard gradient-based approximations. The SFS turbulent diffusion term was modelled as suggested by Knight et al. [28]. Additionally, a constant value of 0.6 was used for turbulent Prandtl number.

The Favre-filtered transport equations were all solved on multi-block body-fitted meshes consisting of hexahedral cells by employing a second-order accurate parallel finite-volume scheme [25,29–31]. In this scheme, the inviscid flux at each cell face was evaluated using limited linear reconstruction and Riemann-solver based flux functions, while the viscous flux was evaluated utilizing a centrally-weighted scheme. A standard, explicit, two-stage, second-order-accurate, Runge–Kutta, time-marching scheme was used to integrate forward in time the non-linear, coupled-system of ordinary differential equations resulting from the finite-volume spatial discretization procedure. Parallel implementation of the solution method was carried out via domain decomposition using the C++ programming language and the MPI (message passing interface)

Please cite this article in press as: N. Shahbazian et al., *Proc. Combust. Inst.* (2014), http://dx.doi.org/10.1016/j.proci.2014.06.132

library. Second-order accuracy of the finite-volume scheme for discretizations on multi-block body-fitted meshes was demonstrated in previous studies [29–31].

3. CSE combustion model

3.1. Chemistry reduction

While many different models have been proposed for chemistry reduction [32], low-dimensional manifold approaches are very appealing for they significantly reduce the complexity of detailed chemistry while retaining its important features. Maas and Pope [33] first proposed such a model by introducing a formal approach to obtaining an intrinsic low-dimensional manifold (ILDM). Trajectory-generated low-dimensional manifold (TGLDM) is another related approach which generates different realizations of chemistry using a prototype flame [34]. For premixed combustion, it has been found that planar one-dimensional (1D) laminar unstrained premixed flames are good candidates for the prototype flame. Chemistry reduction models derived in such a fashion have been termed flame-generated manifold (FGM) [3] and also flame prolongation of ILDM (FPI) [4] methods. The solution of each 1D laminar flame provides a single trajectory in hyper-dimensional composition space. This trajectory starts from the upstream unburnt fuel–air mixture and ends with the equilibrium burnt products downstream of the reaction zone. Different trajectories can be obtained by changing the upstream conditions of the 1D laminar flame simulations so as to cover the boundaries of the realizable domain in the composition space as characterized by element conservation or constrained equilibrium [17,34].

In combustion of CH_4–air for example, one trajectory for a given equivalence ratio can be obtained by solving a 1D laminar premixed flame for a premixed mixture of CH_4, O_2 and N_2. This gives a single trajectory in the composition space which is called the *fundamental* trajectory. This fundamental trajectory for any solution quantity, φ^{1D-FGM}, can be tabulated as a function of a single progress variable, c_1, and used as a reduced chemistry model. For example, in flamelet models based on 1D-FGM or FPI chemistry reduction techniques, the required reaction rates, $\dot{\omega}_k$, for any species, k, can be tabulated and approximated as

$$\dot{\omega}_k(T,\rho,Y_k) \approx \dot{\omega}_k^{1D-FGM}(c_1), \tag{1}$$

where T, ρ, and Y_k are the gaseous mixture temperature, density, and species mass fractions, respectively, and c_1 is an appropriate progress variable. Required species mass fractions can also be tabulated as function of the progress variable. Fiorina et al. [8] has shown that for CH_4–air combustion, a good choice for the progress variable is the normalized sum of the mass fractions of CO and CO_2.

Assuming an adiabatic flame with constant equivalence ratio, the upstream mixture composition can be changed by adding other species such as CO_2 and H_2O, while conserving the number of elements. This results in different chemical kinetic realizations of the flame solutions and generates other trajectories. These trajectories can then be tabulated as a function of at least two progress variables

$$\dot{\omega}_k(T,\rho,Y_k) \approx \dot{\omega}_k^{2D-FGM}(c_1,c_2), \tag{2}$$

where c_1 and c_2 are the two progress variables defining the 2D-FGM. Increasing the number of progress variables can produce more accurate representations of the chemical kinetics. For CH_4–air combustion, normalized mass fractions of CO_2 and H_2O can be used as the two progress variables. Both the production rates and other species mass fractions can be then tabulated as a function of these two progress variables as depicted in Fig. 1.

3.2. Turbulence-chemistry interaction

Assuming the 2D reduced chemistry model of Eq. (2) is exact, a perfect closure for the filtered chemical reaction source terms can be then obtained as

$$\tilde{\dot{\omega}}_k = \int_0^1 \int_0^1 \dot{\omega}_k(c_1^*,c_2^*)\widetilde{P}(c_1^*,c_2^*)\mathrm{d}c_1^*\mathrm{d}c_2^*, \tag{3}$$

where $\widetilde{P}(c_1^*,c_2^*)$ is the joint Favre-filtered PDF of progress variables. A transported PDF approach [11] can be used to solve for this joint PDF; however, this approach is expensive and results in other closure challenges [10]. Also, since the two progress variables are not statistically

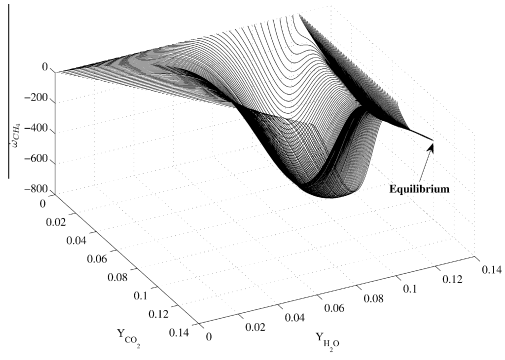

Fig. 1. Illustration of two-dimensional flame-generated manifold (2D-FGM) for methane–air combustion showing the production rate of CH_4 as a function of the progress variables c_1 and c_2.

Please cite this article in press as: N. Shahbazian et al., *Proc. Combust. Inst.* (2014), http://dx.doi.org/10.1016/j.proci.2014.06.132

independent, it is not possible to get the joint PDF by multiplying the marginal PDFs as $\widetilde{P}(c_1^*, c_2^*) \neq \widetilde{P}(c_1^*)\widetilde{P}(c_2^*)$. The conditional closure methods can be used instead which are based on following identity

$$\tilde{\dot{\omega}}_k = \int_0^1 \overline{\dot{\omega}_k|c_1^*}\widetilde{P}(c_1^*)\mathrm{d}c_1^*, \quad (4)$$

where $\overline{\dot{\omega}_k|c_1^*}$ is the conditional rate given $c_1 = c_1^*$ and $\widetilde{P}(c_1^*)$ is the marginal PDF of the reaction progress variable. The conditional reaction rates are related to the conditional PDF of c_2.

3.3. PCM-FPI flamelet model

In the flamelet-based PCM-FPI approach [6–8], the conditional reaction rates, $\overline{\dot{\omega}_k|c_1^*}$, are assumed to be given by those defined by 1D laminar unstrained premixed flame solutions, $\varphi^{\mathrm{1D-FGM}}$, of the fundamental trajectories as described in Section 3.1 above. The marginal PDF is modelled with good accuracy using a presumed shape that is formed by knowing the filtered and subfilter fluctuations of the reaction progress variable [6,19]. While various choices are possible for the presumed marginal PDF of c_1, including β-distributions as commonly used in the modelling of non-premixed combustion, and modified laminar-flame-based PDFs [6,19], Salehi et al. [20] have shown the correctness of the modified laminar flamelet PDF as compared to the β-distribution for premixed flames. In particular, unlike the β-PDF, the modified laminar flamelet PDF is able to recover the filtered laminar flame speed for premixed laminar flames, and is therefore a good choice. Using the 1D-FGM chemistry tabulation and modified laminar flamelet PDF, the final unconditionally-filtered reaction rates are then given by

$$\tilde{\dot{\omega}}_k \approx \int_0^1 \dot{\omega}_k^{\mathrm{1D-FGM}}(c_1^*)\widetilde{P}(c_1^*;\tilde{c}_1,\tilde{c}_{v_1})\mathrm{d}c_1^*, \quad (5)$$

where $\tilde{c}_1$ is the Favre-filtered value of c_1 and $\tilde{c}_{v_1}$ is the subfilter variance of c_1.

The flamelet-based PCM-FPI model as described above was used for comparison to the CSE model solutions. Values of $\tilde{c}_1$ and $\tilde{c}_{v_1}$ were calculated from the progress of reaction, $\widetilde{Y}_{c_1}$, and its SFS variance, $\widetilde{Y}_{c_{v_1}}$, where $\widetilde{Y}_{c_{v_1}} = \widetilde{Y_{c_1}Y_{c_1}} - \widetilde{Y}_{c_1}\widetilde{Y}_{c_1}$. In order to determine $\widetilde{Y}_{c_1}$ and $\widetilde{Y}_{c_{v_1}}$, modelled transport equations for the mean and variance were solved along with the filtered Navier–Stokes equations [35].

3.4. CMC-based CSE model

An alternative approximation of the unconditionally-filtered reaction rates as compared to that provided by the PCM-FPI model of Eq. (5) can be obtained by using the first-order CMC hypothesis [36] in defining the conditional reaction rates. In this case, the conditionally-filtered scalar field is used in defining the reaction rates and one obtains

$$\tilde{\dot{\omega}}_k \approx \int_0^1 \dot{\omega}_k^{\mathrm{2D-FGM}}(c_1^*, \overline{c_2|c_1^*})\widetilde{P}(c_1^*;\tilde{c}_1,\tilde{c}_{v_1})\mathrm{d}c_1^*, \quad (6)$$

where $\overline{c_2|c_1^*}$ is the conditionally-filtered value of c_2 conditioned on c_1, and the 2D-FGM reduced chemistry tabulation procedure defined previously has been used to approximate $\dot{\omega}_k(c_1^*, \overline{c_2|c_1^*})$. In the conventional CMC approach [9], transport equations are solved for $\overline{c_2|c_1^*}$. However as noted above, these transport equations have closure issues, especially in premixed combustion where the coupling between transport and chemistry is strong.

The CSE model [13,14] provides an alternative approach for determining the conditional scalar field, $\overline{c_2|c_1^*}$. This is done in a dynamic fashion by solving the following integral equation

$$\tilde{c}_2(\vec{x}) = \int_0^1 \overline{c_2|c_1^*}(c_1^*;\vec{x})\widetilde{P}(c_1^*;\vec{x})\mathrm{d}c_1^*. \quad (7)$$

In the above equation, $\tilde{c}_2$ is calculated from the progress of reaction, $\widetilde{Y}_{c_2}$ and, for the CSE model, $\widetilde{P}(c_1^*;\vec{x})$ was obtained from the modified laminar flamelet presumed PDF [20]. Assuming that $\overline{c_2|c_1^*}$ is homogeneous (i.e., constant) within an ensemble of points within the computational domain, located on planes at fixed distance from the nozzle, the above integral equation can be discretized and then inverted to obtain $\overline{c_2|c_1^*}$ without the requirement of any additional closure approximations and/or modelling assumptions. Apart from the homogeneity assumption, an implicit assumption in CSE is that the conditionally-filtered value of a scalar can be reconstructed from its unconditionally-filtered value and the statistics of the conditioning variable. Jin et al. [15] showed previously that this assumption is valid in premixed combustion in an *a priori* analysis of DNS data.

3.5. Solution of inverse problem

In the implementation of the CSE model for premixed flames herein, Eq. (7) was discretized using simple quadrature with m bins for c_1^*. For ensembles consisting of a collection of n hexahedral computational cells within the domain, the inverse problem can then be re-expressed following the application of a simple midpoint quadrature rule for the integration over progress variable space as the linear system of equations,

$$\vec{b} = \mathbf{A}\vec{\alpha}, \quad (8)$$

requiring solution where $b_j = \tilde{c}_2(\vec{x}_j)$ for $j = 1:n$ and α_i for $i = 1:m$ contains the discrete form of the solution for $\overline{c_2|c_1^*}$. The matrix, $\mathbf{A}$, is called the *design* matrix and its elements were calculated

Please cite this article in press as: N. Shahbazian et al., *Proc. Combust. Inst.* (2014), http://dx.doi.org/10.1016/j.proci.2014.06.132

here from integration of the modified laminar flamelet PDF in each bin for every point in the ensemble.

The linear system arising from the inverse problem can be in many cases poorly conditioned. To deal with this issue, a Tikhonov regularization approach [37] can be used to obtain the solution as given by

$$\vec{\alpha}^{*} = \arg\min_{\vec{\alpha}} \left(||\mathbf{A}\vec{\alpha} - \vec{b}||_2^2 + \lambda^2 ||\vec{\alpha} - \vec{\alpha}^0||_2^2 \right), \qquad (9)$$

where $\vec{\alpha}^0$ is a target solution based on *a priori* knowledge of the solution and λ is the regularization parameter. For the premixed flames of interest here, Tikhonov regularization was used and $\vec{\alpha}^0$ was taken to be the fundamental 1D laminar premixed flame solutions, $\varphi^{\mathrm{1D-FGM}}$. In this way, CSE is then capable of recovering flamelet solutions in the flamelet regime. Additionally, the L-curve method was used to find an optimum value for the regularization parameter, λ, at each ensemble [38].

Note that the CSE inverse problem as defined above is linear in each time step. Nevertheless, the solution of the inverse problem in one time step affects both the design matrix and vector $\vec{b}$ in the next step. Therefore, the inverse problem is non-linear over consecutive time steps. The stability of a non-linear inverse problem cannot be determined easily and numerical experiments are required to demonstrate this property. As such, an important objective of this research is to show via numerical experiment the stability and convergence of the CSE model for LES of premixed flames.

4. Premixed burner setup and measurements

As part of the assessment of the CSE combustion model for premixed flames, LES predictions were considered for two laboratory-scale Bunsen-type turbulent premixed methane–air flames examined previously in the experimental work by Yuen and Gülder [24]. The burner for both flames was an axisymmetric Bunsen type with an inner nozzle diameter, D, of 11.2 mm. The turbulent flames were stabilized by annular pilot flames.

Flame front images were captured using planar Rayleigh scattering with a resolution of 45μm/pixel. The Rayleigh scattering images were converted to a temperature field and then post-processed to attain instantaneous and time-averaged 2D distributions of the temperature gradient and progress variable based on temperature. Additional two-dimensional maps of the flame surface density (FSD) were computed using the method developed by Shepherd [39]. Distributions of the FSD and 2D flame curvature were also determined. A total of 300 experimental images were used in post-processing of the experimental data for each flame. To compare fairly the experimental results to time-averaged LES predictions, the experimental images were filtered using a top-hat filter with a characteristic size equal to the LES filter width as first proposed by Hernández Pérez et al. [25]. This was necessary because the Rayleigh measurements were carried out with a higher resolution than the corresponding LES simulations. In addition, the instantaneous velocity field was also measured using particle image velocimetry (PIV) technique.

The two experimental cases of Yuen and Gülder [24] considered here were the stoichiometric (equivalence ratio, $\phi = 1$) and lean ($\phi = 0.7$) CH_4–air premixed flames with relative turbulence intensities of $u'/s_L = 7.25$ and 14.38, where s_L is the laminar flame speed. The two flames, referred to here as flame A and flame B, respectively, both had a burner inlet mean velocity of 15.58 m/s. These two flames, with Karlovitz numbers of 3.26 and 13.73, respectively, lie well within the thin-reaction zones region of the standard premixed flame regime diagram [12].

5. LES results and discussion

A cylindrical computational domain having a diameter of 0.05 m and a height of 0.1 m was employed for the LES simulations of the two premixed flames. In both cases, a grid consisting of 1,638,400 hexahedral cells was used. For CSE, the grid was decomposed to create 800 ensembles, each with 2,048 cells, that were used in the solution of the inverse problem for the conditionally-filtered progress variable. The pilot flame was approximated by a uniform inflow of combustion products surrounding the inlet inflow at a velocity of 16.81 m/s. For the turbulent inflow at the exit of the nozzle, a uniform (flat-top) mean inflow profile of reactants is superimposed onto a turbulent field that was convected into the computational domain. The homogeneous isotropic turbulent field at the inflow was pre-generated using the procedure of Rogallo [40] along with the model spectrum of Haworth and Poinsot [41].

The turbulence intensity at the burner inlet was reported to be 2.92 m/s for both flames A and B. However, the measured intensity did not take into account the entire inlet profile. Measurements were limited to a region close to the centreline of the burner. More recently, experiments performed in the same burner have shown that the turbulence intensity is not uniform and is greater in the shear layer near the burner rim than closer to the centreline (private communication, P. Tamadonfar, 2013). Furthermore, the shape of the radial distributions of normalized turbulence intensity was found to be virtually identical for different levels of turbulence intensity. As it is expected that the flames are stabilized in the regions of higher turbulence near the burner rim [42], the prescribed

Please cite this article in press as: N. Shahbazian et al., *Proc. Combust. Inst.* (2014), http://dx.doi.org/10.1016/j.proci.2014.06.132

uniform turbulence intensity at the inlet in the LES was increased above the nominal reported value in an attempt to represent more accurately the actual inflow turbulence. The prescribed value for the inflow turbulence in the LES was taken to be higher than the midplane value recorded in the experiments by 75% of the difference between the peak and centreline values. As a result, a value of 3.78 m/s was used for both flames.

5.1. Instantaneous flame front

Three-dimensional views of the predicted instantaneous iso-surfaces of the filtered progress variable, $\tilde{c}_T = 0.5$, for flames A and B obtained using both the PCM-FPI and CSE models are depicted in Fig. 2, corresponding to $t = 9$ ms after the initiation of the simulation. At this time, a quasi-steady flame structure has been achieved in each case. Isolated pockets of unburnt reactants can be identified higher in the flames.

A first important observation from the results of Fig. 2 is that the proposed formulation of the CSE model for LES is stable and converges to what appear to be physically reasonable solutions for the flames of interest. In general, the simulated flames have highly wrinkled surfaces, with similar wrinkling for both PCM-FPI and CSE models. The estimated instantaneous heights of both flames would also appear to be alike for CSE and PCM-FPI predictions. Moreover, both SFS models result in slightly shorter flames for the stoichiometric case compared to the lean flame, as was observed in the experiments.

5.2. Conditionally-filtered progress variable

It is instructive to examine the results of the CSE inversion for these flames. The predicted instantaneous distributions of the conditionally-filtered progress variable, $\overline{c_2|c_1^*}$, within five chosen ensembles for lean flame B ($\phi = 0.7$) at $t = 9$ ms are shown in Fig. 3. Results for flame A are similar. For the ensembles located lower in the flame (non-dimensional height z/D small where z is the height above the burner), it is evident that the conditional averages, $\overline{c_2|c_1^*}$, deviate considerably from the flamelet solution whereas, higher up in the flame, the conditionally-filtered progress variable converges to the flamelet solution. This is likely due to the fact that the turbulence in the burner was generated using a grid and such turbulence decays downstream of the grid [43,44]. While the actual conditional averages were not measured in the experiment, this type of behaviour where the conditional averages tend to a straight line for high turbulence intensities was observed in a recent DNS study of premixed flame in the distributed reaction zone regime [45]. This interpretation of the CSE results can be further justified by considering the predicted solutions for strained laminar flamelets in a opposed-jet counter-flow burner configuration for a lean ($\phi = 0.7$) methane–air mixture as shown in Fig. 4. It is clear that strained flamelet solutions deviate from that of the unstrained flamelet with increasing strain rate, S, and approach a straight-line profile in a similar fashion to that of the predictions for the conditional averages described above.

5.3. Time-averaged flame structure

Further comparisons of the predicted structure of the Bunsen flames obtained using each of the two models are shown in Fig. 5, where planar cross sections of the time-averaged temperature field, $\overline{T}$, are shown. About 20 instantaneous

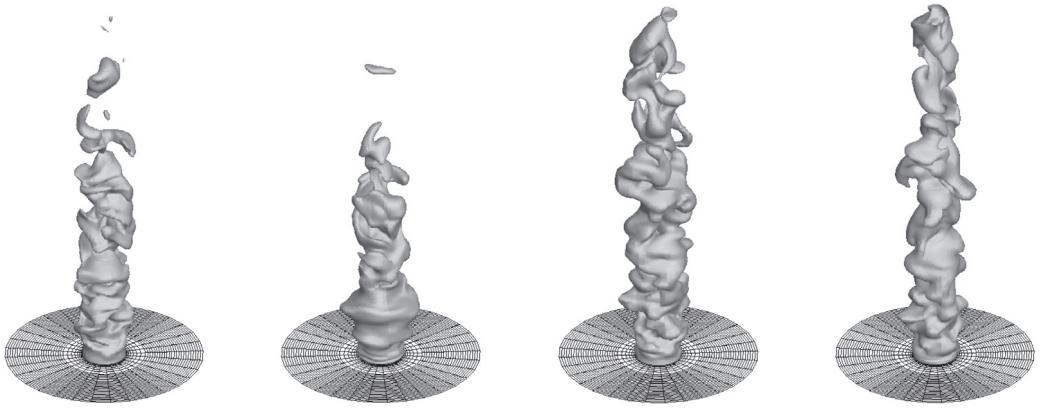

(a) PCM-FPI, flame A (b) CSE, flame A (c) PCM-FPI, flame B (d) CSE, flame B

Fig. 2. Instantaneous iso-surfaces of the filtered progress variable, $\tilde{c}_T = 0.5$, at $t = 9$ ms after the initiation of the simulations for flames A and B obtained using both PCM-FPI and CSE combustion models.

Please cite this article in press as: N. Shahbazian et al., *Proc. Combust. Inst.* (2014), http://dx.doi.org/10.1016/j.proci.2014.06.132

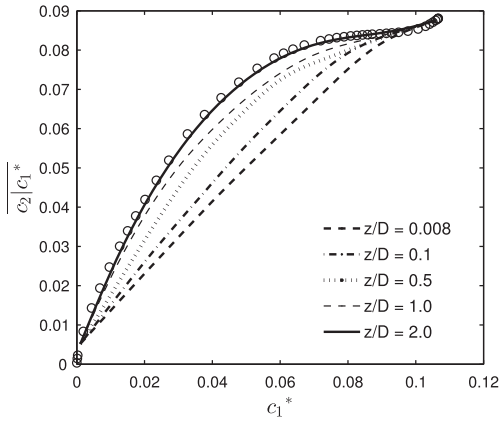

Fig. 3. Predicted distributions of the conditionally-filtered progress variable, $\overline{c_2|c_1^*}$, within the ensembles for lean flame B ($\phi = 0.7$) at $t = 9$ ms; solid lines are the CSE model results as a function of the non-dimensional height in the flame, z/D, and the symbols represent the fundamental unstrained laminar flamelet solution.

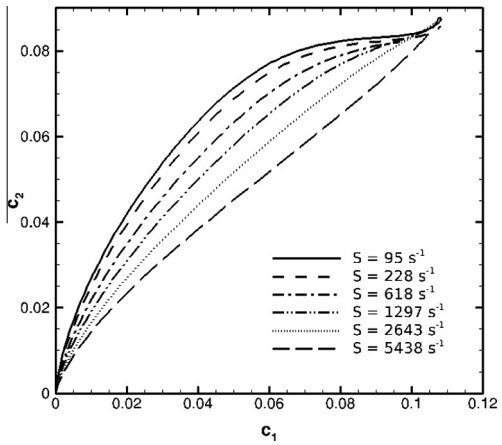

Fig. 4. Strained laminar flamelet solutions for a lean ($\phi = 0.7$) methane–air mixture showing c_2 versus c_1 as a function of strain rate, S, in an opposed-jet counter-flow burner configuration.

distributions of the predicted temperature separated by 0.25 ms time intervals were averaged to obtain the two-dimensional results for the time-averaged temperature. The longer flame structure of the lean mixture is fairly evident in the figure.

5.4. Flame surface density and curvature

Distributions of the 2D FSD as a function of the progress variable, $\bar{c}_T$, as extracted from the Rayleigh measurements for the two flames, are compared directly to the similarly processed LES solutions in Fig. 6a for stoichiometric flame A. Comparisons of the measured and predicted PDFs of the 2D flame front curvature corresponding to a progress variable $\bar{c}_T = 0.5$ are also given in Fig. 6b for this flame. Numerical results for both the CSE and PCM-FPI models are shown. While not shown, similar results were obtained for flame B. From Fig. 6a, one can see that, in general, the predicted distributions of FSD agree well with the experimental results and, despite some quantitative discrepancies, at least qualitatively reproduce the observed trends. In all of the profiles, the maximum value for the FSD is around $\bar{c}_T = 0.5$. Moreover, the peak FSD value obtained from the simulations matches well with the experimental values, with a slight under-prediction by the CSE model. The results of the figure also provide further support for the slightly decreased flame wrinkling in the LES solutions with the CSE model as compared to that of the PCM-FPI model.

From the comparisons of the measured and predicted PDFs of Fig. 6b, it is apparent that both the experimental and numerical PDFs are symmetric about zero and have Gaussian-type distributions. While the curvature PDFs obtained from the LES predictions are somewhat narrower as compared to those for the experiments due to the filtered nature of the LES solutions and the possible lack of grid resolution for high curvature content, overall the predicted distributions of curvature for both combustion models are remarkably similar and agree well with the filtered experimental results.

5.5. Flame height

Predictions of the average map of $\bar{c}_T = 0.5$, representing the average flame envelope, for PCM-FPI and CSE models are compared with the similar map obtained from the Rayleigh scattering images in Fig. 7. Results for both flames A and B are given. The maps are indicative of the overall flame heights. It is apparent from the results that, overall, the two combustion models yield flame heights that agree reasonably well with the experimental values in both cases, particularly given that the uncertainties in the accurate specification of the upstream turbulence discussed previously is estimated to translate to a 10% uncertainty in flame height predictions. For both flames, the agreement between the LES predictions and experiment is very good. The CSE approach is stable and is able to produce solutions that agree well with the PCM-FPI model and the experiments. Moreover, it is felt that the CMC-based CSE model is able to represent better the observed variations in flame height (slightly less differences in predicted flame height between stoichiometric and lean flames as in experiment), yielding taller flames than the flamelet-based model due to the lower predicted burning rates arising from the regions of high turbulent strain.

Please cite this article in press as: N. Shahbazian et al., *Proc. Combust. Inst.* (2014), http://dx.doi.org/10.1016/j.proci.2014.06.132

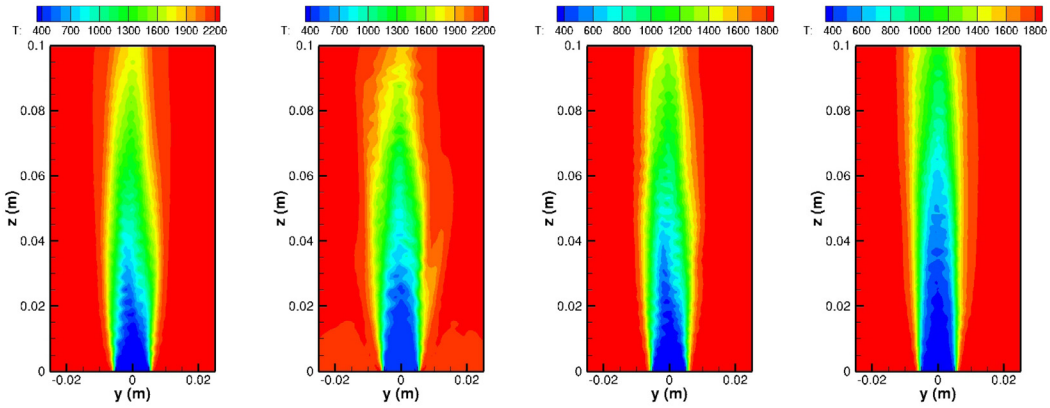

(a) PCM-FPI, flame A (b) CSE, flame A (c) PCM-FPI, flame B (d) CSE, flame B

Fig. 5. Predicted time-averaged temperature field, $\overline{T}$, for flames A and B obtained using both PCM-FPI and CSE models.

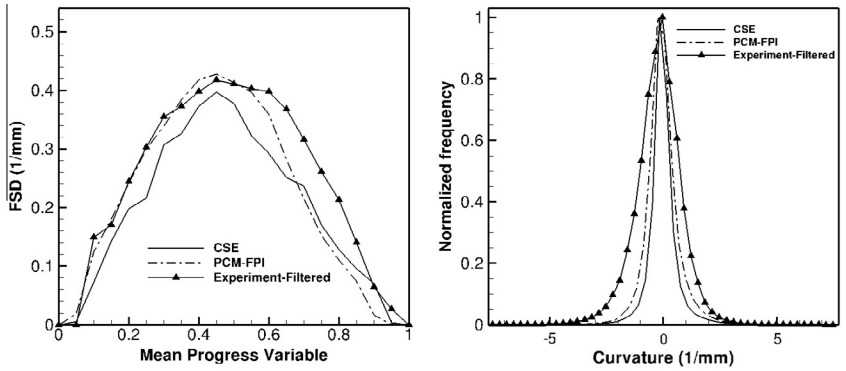

(a) (b)

Fig. 6. Distributions of 2D FSD and PDFs of 2D flame front curvature corresponding to a value for the progress variable of $\tilde{c}_T = 0.5$ as extracted from experimental Rayleigh images and LES results based on instantaneous planar distributions of temperature for flame A.

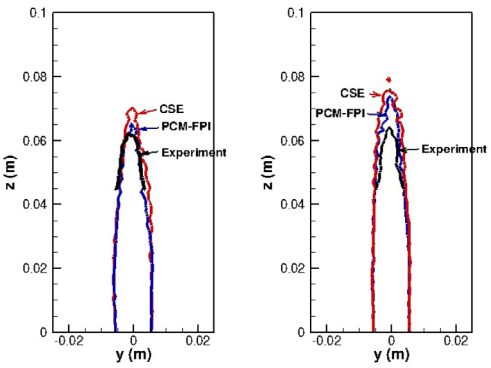

(a) flame A (b) flame B

Fig. 7. Estimated averaged flame envelope for flames A and B based on $\tilde{c}_T = 0.5$ contour of time-averaged progress variable map.

6. Concluding remarks

The conditional source-term estimation combustion model has been formulated for LES of turbulent premixed flames and applied for the first time to the prediction of two laboratory-scale premixed flames identified to lie within the thin reaction zones regime. The CSE model was coupled to a 2D-FGM chemistry reduction model and the modified laminar flamelet presumed PDF, and the LES predictions of lean and stoichiometric methane–air Bunsen-type flames were examined. Comparisons were made to available experimental data, as well as to the predictions of the flamelet-base PCM-FPI combustion model. The CSE combustion model was found to be stable and converge to physically meaningful results. The deviations of the CSE predictions from flamelet

Please cite this article in press as: N. Shahbazian et al., *Proc. Combust. Inst.* (2014), http://dx.doi.org/10.1016/j.proci.2014.06.132

behaviour were identified and attributed to regions of high turbulence intensity and strain for the thin-reaction-zones-regime flames. In general, the CSE model predicted a slightly less wrinkled flame with a lower turbulent burning rate and, consequently, a slightly higher flame height compared to the PCM-FPI model. Overall, it is felt that this CMC-based model would seem to provide rather good predictions that agree both qualitatively and quantitatively with the observed flame behaviour. While the results of the present study are promising, further improvements to the modelling should be explored, including the more accurate specification of the burner inlet flow conditions, use of more accurate SFS turbulence modelling, and improved treatments of the chemistry (the reduced chemistry model adopted herein is still flamelet-based). The application and assessment of the CSE model for a wider range of premixed flames and burner configurations should also be explored.

References

[1] B.F. Magnussen, B.H. Hjertager, *Proc. Combust. Inst.* 16 (1976) 719–729.
[2] O. Colin, F. Ducros, D. Veynante, T. Poinsot, *Phys. Fluids* 12 (2000) 1843–1863.
[3] J.A. van Oijen, L.P.H. de Goey, *Combust. Sci. Tech.* 161 (2000) 113–137.
[4] O. Gicquel, N. Darabiha, D. Thévenin, *Proc. Combust. Inst.* 28 (2000) 1901–1908.
[5] J.A. van Oijen, F.A. Lammers, L.P.H. de Goey, *Combust. Flame* 127 (2001) 2124–2134.
[6] P. Domingo, L. Vervisch, S. Payet, R. Hauguel, *Combust. Flame* 143 (2005) 566–586.
[7] B. Fiorina, O. Gicquel, L. Vervisch, S. Carpentier, N. Darabiha, *Combust. Flame* 140 (2005) 147–160.
[8] B. Fiorina, O. Gicquel, L. Vervisch, S. Carpentier, N. Darabiha, *Proc. Combust. Inst.* 30 (2005) 867–874.
[9] A.Y. Klimenko, R.W. Bilger, *Prog. Energy Combust. Sci.* 25 (1999) 595–687.
[10] S.B. Pope, *Prog. Energy Combust. Sci.* 11 (1985) 119–192.
[11] P. Givi, *Prog. Energy Combust. Sci.* 15 (1989) 1–107.
[12] N. Peters, *Turbulent Combustion*, Cambridge University Press, 2000.
[13] W.K. Bushe, H. Steiner, *Phys. Fluids* 11 (1999) 1896–1906.
[14] H. Steiner, W.K. Bushe, *Phys. Fluids* 13 (2001) 754–769.
[15] B. Jin, R. Grout, W.K. Bushe, *Flow Turbul. Combust.* 81 (2008) 563–582.
[16] M.M. Salehi, W.K. Bushe, K.J. Daun, *Combust. Theory Modell.* 16 (2012) 301–320.
[17] J. Huang, W.K. Bushe, *Combust. Theory Modell.* 11 (2007) 977–1008.
[18] M. Wang, J. Huang, W.K. Bushe, *Proc. Combust. Inst.* 31 (2007) 1701–1709.
[19] M.M. Salehi, W.K. Bushe, *Combust. Theory Modell.* 14 (2010) 381–403.
[20] M.M. Salehi, W.K. Bushe, N. Shahbazian, C.P.T. Groth, *Proc. Combust. Inst.* 34 (2013) 1203–1211.
[21] R.W. Grout, W.K. Bushe, C. Blair, *Combust. Theory Modell.* 11 (2007) 1009–1028.
[22] M. Wang, W.K. Bushe, *Phys. Fluids* 19 (115103) (2007) 1–12.
[23] D. Dovizio, M.M. Salehi, C.B. Devaud, *Combust. Theory Modell.* 17 (2013) 935–959.
[24] F.T.C. Yuen, O.L. Gülder, *Proc. Combust. Inst.* 32 (2009) 1747–1754.
[25] F.E. Hernández-Pérez, F.T.C. Yuen, C.P.T. Groth, O.L. Gülder, *Proc. Combust. Inst.* 33 (2011) 1365–1371.
[26] S. Gordon, B.J. McBride, Reference Publication 1311, NASA, 1994.
[27] A. Yoshizawa, K. Horiuti, *J. Phys. Soc. Jpn.* 54 (1985) 2834–2839.
[28] D. Knight, G. Zhou, N. Okong'o, V. Shukla, Paper 98-0535, AIAA, 1998.
[29] X. Gao, C.P.T. Groth, *Int. J. Comput. Fluid Dyn.* 20 (5) (2006) 349–357.
[30] X. Gao, C.P.T. Groth, *J. Comput. Phys.* 229 (2010) 3250–3275.
[31] X. Gao, S.A. Northrup, C.P.T. Groth, *Prog. Comput. Fluid Dyn.* 11 (2) (2011) 76–95.
[32] J. Warnatz, U. Maas, R. Dibble, *Combustion*, Springer, 2000.
[33] U. Maas, S.B. Pope, *Combust. Flame* 88 (1992) 239–264.
[34] S.B. Pope, U. Maas, Paper FDA 93-11, Cornell University, 1993.
[35] P. Domingo, L. Vervisch, D. Veynante, *Combust. Flame* 152 (2008) 415–432.
[36] R.W. Bilger, *Phys. Fluids A* 5 (1993) 436–444.
[37] A. Tikhonov, V. Arsenin, *Sov. Math. Dokl.* 4 (1963) 1035–1038.
[38] P.C. Hansen, *Inverse Probl.* 8 (1992) 849–872.
[39] I. Shepherd, *Proc. Combust. Inst.* 26 (1996) 373–379.
[40] R.S. Rogallo, NASA Technical Memorandum 81315, 1981.
[41] D.C. Haworth, T.J. Poinsot, *J. Fluid Mech.* 244 (1992) 405–436.
[42] K. Herrmann, *Strömung, Flammencharakterisierung und Stickoxid-bildung in Turbulrnten Vormischflammen*, Ph.D. thesis, ETH Zürich, 2002.
[43] S.B. Pope, *Turbulent Flows*, Cambridge University Press, 2000.
[44] P. Siewert, *Flame Front Characteristics of Turbulent Lean Premixed Methane/Air Flames at High-pressure*, Ph.D. thesis, ETH Zurich, 2006.
[45] A.J. Aspden, M.S. Day, J.B. Bell, *Proc. Combust. Inst.* 33 (2011) 1463–1471.

Please cite this article in press as: N. Shahbazian et al., *Proc. Combust. Inst.* (2014), http://dx.doi.org/10.1016/j.proci.2014.06.132